Hindawi
Mathematical Problems in Engineering
Volume 2022, Article ID 4249726, 9 pages
https://doi.org/10.1155/2022/4249726

Research Article

DEM Investigation of Discrete Heat Transfer Behavior of the Grinding Media in Ball Mills

Zixin Yin,[1,2] **Nan Wang**,[1,2] **and Tongqing Li**[3]

[1]*School of Mechanical and Electronic Engineering, Suzhou University, Suzhou 234000, China*
[2]*Suzhou University Technology and Research Center of Engineering Tribology, Suzhou University, Suzhou234000, China*
[3]*School of Mechanical Engineering, Jiangsu Ocean University, Lianyungang 222005, China*

Correspondence should be addressed to Zixin Yin; yzxszu@126.com and Nan Wang; szxywn@126.com

Received 29 March 2022; Accepted 31 May 2022; Published 30 July 2022

Academic Editor: Ardashir Mohammadzadeh

This study presented a numerical model for the quantitative assessment of the heat transfer behavior of grinding media inside a ball mill. Effects of various mill speeds, grinding media filling, and the number of lifters on heat transfer were studied and verified by comparing the experimental results and the numerical simulations calculated by DEM (Discrete Element Method). The results show that the heat transfer of grinding media has a strong sensitivity to the variation of the mill speed, grinding media filling, and the number of lifters. The optimum grinding conditions for heat transfer behavior can be determined in terms of the temperature field of the grinding media. The maximum temperature rise of grinding media occurs at a range from 70% to 80% of critical speed. The maximum average temperature of grinding media up to 295.057 K appears at the grinding media filling 25% and the number of lifters 12. Subsequently, validation experiments are carried out to validate the numerical simulation results. The experimental results are closer to the simulation results, indicating the reasonability of the heat transfer model.

1. Introduction

Ball mills are widely used in many industrial fields for grinding and crushing granular materials, such as the mineral, chemical, and pharmaceutical industries [1–4]. It is dependent on the lifters to lift the grinding media to a specific level of energy and the balls then cataract and cascade, and in consequence, collide with each other, resulting in particles breakage. As a very complicated system, ball mills are typically high-energy and inefficient equipment because of the environment itself. To this end, it is worth attempting to reduce the energy consumption of the ball mill by any means [5].

The charge motion, liner wear, and particle breakage behavior in ball mills have been attracted considerably further attention [6–8]. These outstanding results provide a sound foundation for optimizing mill performance and reducing energy consumption. In the grinding process, bulk ore particles in the grinding process lead to elevated temperatures of the milling environment. This in turn will influence the particle breakage behavior and the energy consumption of the ball mills, such as tantalum ore particles. However, there are comparatively few studies on heat transfer in conjunction with particle collisions in ball mills. One of the challenges involved in understanding the heat transfer is the approach to determining the temperature distribution of the grinding media in ball mills.

Heat transfer in granular materials is a common phenomenon, and it affects a wide variety of applications ranging from food products to building materials. The phenomenon of heat transfer inside a rotating drum is widely encountered in areas ranging from food products to building materials. In recent years, alternative methodologies have been used to study the heat transfer phenomena, including kinetic theory [9], continuum approaches [10–13], and DEM simulation [14–17]. Chaudhuri et al. [18] used the method of experimentation and DEM simulation to examine the flow, mixing, and mass and heat transport in rotary calciners. Alumina and copper were used to understand the effect of particle flow and heat transfer on the calcination performance. The results showed that the material with higher thermal conductivity

warmed up faster in experiments and DEM simulations. Xie et al. [19] investigated the heat transfer inside a drum mixer by coupling the DEM simulation with a conductive heat transfer model. The DEM simulation showed that the specific heat transfer coefficient of the particle flow increased with the increasing rotating speed but decreased with the amounts and heights of the lifters. Komossa et al. [20] investigated the heat transfer in an indirectly heated tumbling drum. The particle movement and heat transfer showed a good agreement between the DEM simulation and the experiment. Gui and Fan [21] used the DEM simulation with a thermal conduction model to investigate the effects of the rotation speed and the wave number on the heat transfer. The wavy drums raised the heat transfer process higher than a circular drum for a lower rotation speed. Figueroa et al. [22] applied various evaluation methods to examine the interaction between heat transfer and particle load behavior. A continuum model was used to study the relationship between temperature contours and mixing patterns. Oschmann et al. [23] derived a novel particle-wall heat transfer coupling algorithm from resolving the heat transfer due to particle-wall contact and inner wall heat conduction. Li et al. [24] studied the heat transfer of granular material in a rotary drum. The results showed that increasing rotational speed can intensify heat transfer to a certain degree, and the average temperature of granular materials increases with the number of flights and decreases the fill level. These above-mentioned studies have provided an understanding of the heat transfer phenomena of granular materials. The drums and granular materials are preheated before grinding and mixing, which is completely different from the grinding process of ball mills. In addition, the heat generated by the granular particle collision is not taken into account.

This paper provides a novelty DEM heat transfer model to investigate the multibody collision in the ball mills. The effects of the mill speed, grinding media filling, and the number of lifters on the temperature field of grinding media are further studied. A laboratory-scale ball mill is employed to perform measurements and validate numerical results.

2. Heat Transfer Model

The heat transfer involved within the particles includes thermal convection, thermal radiation, and thermal conduction, as shown in Figure 1. To quantitatively describe the discrete heat transfer behavior of the grinding media in ball mills, the thermal conduction, and collisional heat of the heat transfer model are considered while the convection and the radiation are being ignored [19]. In this model, the following assumptions are considered:

(1) The ball mill temperature remains unchanged, and there is no thermal exchange between the particles and the geometry

(2) The heat generated due to friction can be neglected

(3) Only the heat transfer in the particle flow due to the contact conduction and collision effect is considered, and the interstitial gas is neglected

(4) The thermal-physical properties of the grinding media and the iron ore are constant

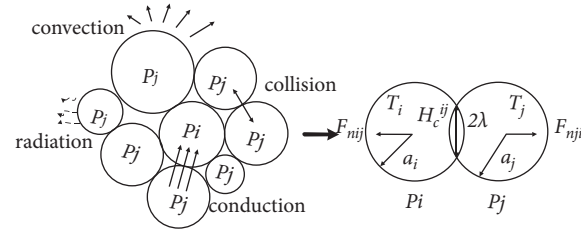

Figure 1: Schematic of heat transfer.

In the DEM simulation software, the granular materials are considered as a collection of frictional inelastic spherical particles. A nonlinear Hertz–Mindlin no-slip model is employed to solve the contact force between colliding particles. In DEM simulations, the forces and torques acting on a particle i can be expressed as follows:

$$\begin{aligned} m_i a_i &= \sum F, \\ I_i \theta_i &= \sum M, \end{aligned} \tag{1}$$

where m_i, I_i, a_i, and θ_i are, respectively, the mass, moment of inertia, acceleration, and angular acceleration of particle i; $\sum F$ and $\sum M$ are the total force and torque applied on particle i, respectively.

The normal contact and tangential contact forces between particles i and j can be described as follows:

$$\begin{aligned} F_n &= -K_n \Delta x + C_n v_n \\ F_t &= \min\left\{ u F_n, K_t \int v_t dt + C_t v_t \right\}. \end{aligned} \tag{2}$$

where K_n and K_t are the normal and tangential stiffness, respectively; $\triangle x$ is the amount of overlap; v_n and v_t are the normal and tangential relative velocity, respectively; C_n and C_t are the normal and tangential damping coefficient, respectively; u is the friction coefficient.

The C_n depends on the coefficient of restitution ε, which is given by the following equation:

$$C_n = -2 \ln(\varepsilon) \frac{\sqrt{m_{ij} K_n}}{\sqrt{\pi^2 + \ln^2(\varepsilon)}}, \tag{3}$$

where $m_{ij} = m_i m_j / m_i + m_j$.

The total heat dissipation of the particle I can be written as follows:

$$Q_i = m_i C_i \frac{dT_i}{dt} = \sum_{j=1}^{N} \left(H_c^{ij} \left(T_i - T_j \right) + Q_c^{ij} \right). \tag{4}$$

The H_c^{ij} is a function of the compression force, which refers to the ability of two materials in contact to transfer heat through their mutual interface, which can be expressed as follows [25]:

$$H_c^{ij} = 2 k_p \lambda = \frac{4 k_{p1} k_{p2}}{k_{p1} + k_{p2}} \left[\frac{3 F_n a^*}{4 E^*} \right]^{1/3}, \tag{5}$$

where C_i is the specific heat capacity of particle i, T_i, and T_j are the temperatures of particle i and j, respectively, H_c^{ij} is

Table 1: Ball mill parameters.

Parameters	Test 1	Test 2	Test 3
Mill speed ψ (of critical speed)	50%, 60%, 70%, 80%, 90%, 100%	75%	75%
Grinding media filling J	25%	10%, 15%, 20%, 25%, 30%, 35%	25%
Number of lifters n	12	12	0, 8, 12, 16

the heat transfer coefficient between particles i and j with j varying from 1 to the contact number N, k_p is the thermal conductivity of the granular media, λ represents the contact radius, F_n is the normal force, a^* is the equivalent radius, and E^* is the effective Young's modulus.

The Q_c^{ij} is the heat dissipation by particle collision, which can be expressed as follows:

$$Q_c^{ij} = k\beta E_{ij}, \tag{6}$$

where k refers to the proportional coefficient of collision loss energy converted into internal energy, $k = 0.97$ [26, 27], β is the heat flux distribution coefficient, and E_{ij} is the collision loss energy.

3. Materials and Methods

In this paper, the laboratory-scale ball mill of 520 mm diameter and 260 mm length is employed to investigate the effects of mill speed, grinding media filling, and the number of lifters on the temperature field of the grinding media. The ball mill parameters and its DEM simulation parameters are listed in Tables 1 and 2 [27].

4. DEM Simulation Results and Discussions

4.1. Effect of Mill Speed. Mill speed is one of the vital parameters in ball mills, and it is normally specified as a fraction of critical speed. It determines whether the load behavior is predominantly the cascading regime, the cataracting regime, or the centrifuging regime. Figure 2 shows the effect of mill speed on the temperature field of the grinding media. As shown in Figure 2, significant differences in the temperature field of the grinding media can be observed at different mill speeds. The difference in the colors refers to the temperature of the grinding media, red for the highest temperature and blue for the lowest. As the mill speed is increased from 50% to 100%, a larger amount of grinding media are lifted, and the load behavior has changed from the cataracting regime to the centrifuging regime. This result indicates a dependency of the temperature field of the grinding medium on the loading behavior.

In addition, the load behavior remains nearly unchanged at the mill speed of 50% to 60%, whereby the grinding media is being increasingly lifted to a higher position at mill speeds of 70% to 80%. The temperature field is accordingly altered. As the mill speed reaches 90%–100%, the outermost layer of the grinding media undergoes centrifugation, while the inner layer moves with a cascading regime, exhibiting a significant temperature difference. This is due to a larger amount of grinding media being lifted, reducing heat transfer and contact behavior. In summary, mill speed has a significant effect on heat transfer, and the change in the temperature field of grinding media indicates the intensity of charge motion.

To quantify the effect of mill speed on the temperature field of the grinding media, the particle numbers at different temperatures are performed, as shown in Figure 3. The results show that the maximum particle number corresponds to the grinding media temperatures for various mill speeds are 298.043 K, 298.048 K, 298.055 K, 298.057 K, 298.049 K, and 298.021 K, respectively. In addition, the average temperature of grinding media increases first and then decreases with mill speed. With a mill speed of 50% of the critical speed, the range of grinding media temperatures is relatively more minor due to the lower mill speed, which leads to the grinding media in cascading motion. With a mill speed of 60% of critical speed, the range of grinding media temperatures is much greater than that at $\psi = 50\%$. The grinding media temperature distribution of the grinding media is dispersed, and the grinding media temperature increases. This changes because the grinding media is lifted and mixed. With a mill speed of 70% of the critical speed, most grinding media is concentrated at a higher temperature. The range of temperatures is minimal compared with the other condition of the mill speeds. This indicates that the mill speed significantly affects the grinding media temperature rise. With a mill speed of 80% of critical speed, there is a similar tendency to at $\psi = 70\%$, but the main change is that the grinding media temperature is marginally lower. However, at a higher speed of $\psi = 90\%$–100%, the grinding media is trapped between lifters and progressively deviates to the centrifugal motion, resulting in the wide distribution of grinding media temperature. The above-given cases indicate that the mill speed affects the load behavior and the temperature rise, and the maximum grinding media temperature rise is between $\psi = 70\%$–80%.

4.2. Effect of Grinding Media Filling. The particle breakage process is performed by falling grinding media in ball mills. The crushing and the grinding intensity of the ore particles are dependent on the grinding media amount and velocity. The grinding media filling is a significant operating factor affecting particle breakage and load behavior [28]. The amount of grinding media in the ball mill affects the load behavior and the heat transfer. The current research mainly involves observing the heat transfer phenomenon of the particles by heating the rotating body. However, there has been no reporting on the variation of the temperature field of grinding media with different grinding media fillings. To understand the interrelation between the grinding media filling and the temperature field of grinding media, for the ball mill, grinding media fillings for six levels between $J = 10\%$ and $J = 35\%$ are selected, as shown in Figure 4. All the

Table 2: DEM simulation parameters.

Parameters		Value
Grinding media	Size (mm)	30
	Initial temperature (K)	298
	Poisson's ratio	0.30
	Specific heat capacity (J/kg ∗ K)	598.60
	Thermal conductivity (W/m ∗ K)	55.90
	Thermal diffusion coefficient (cm^2/s)	0.12
	Shear modulus (Pa)	7e+10
	Density (kg/m^3)	7850
Coefficient of restitution	Grinding media—grinding media	0.75
	Grinding media—wall	0.45
Coefficient of rolling friction	Grinding media—grinding media	0.01
	Grinding media—wall	0.01

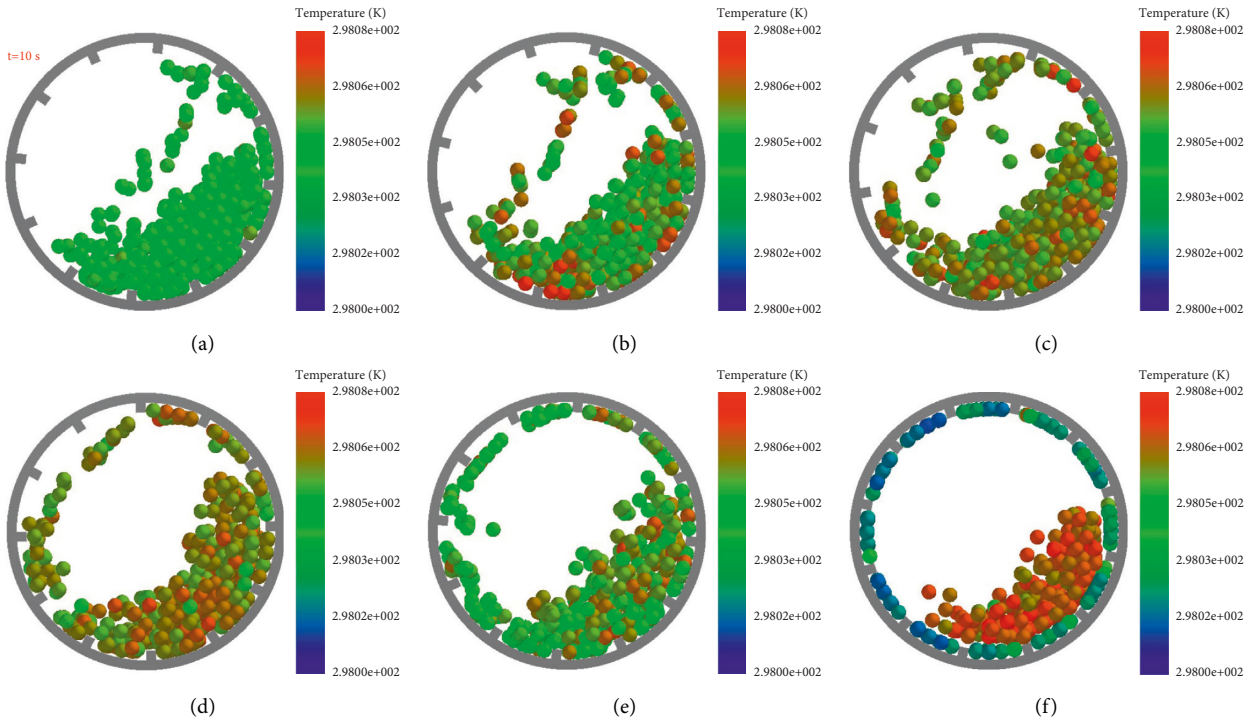

Figure 2: Effect of mill speed on the temperature field of grinding media. (a) $\psi = 50\%$. (b) $\psi = 60\%$. (c) $\psi = 70\%$. (d) $\psi = 80\%$. (e) $\psi = 90\%$. (f) $\psi = 100\%$.

load behavior shows that the toe and shoulder angles of the grinding media remain almost unchanged, but the significant difference is the cascading free surface. The grinding media distribution presents obviously two parts of cataracting and cascading. More grinding media is lifted, and the amount of grinding media cascading down from the bulk of grinding media increases with the grinding media filling. At $J = 10\%–15\%$, the grinding media mainly have a green color. As the grinding media filling increases from 20% to 35%, it is clearly displayed that the red grinding media are more than that of the lower grinding media filling. However, the temperature field of grinding media only changes slightly.

Figure 5 shows the average grinding media temperature variation for different grinding media fillings, which corresponds to the temperature field of grinding media in Figure 4. As the ball mill motion tends toward a steady state, the average grinding media temperature increases to a maximum value at $J = 25\%$, decreasing from $J = 30\%$ to $J = 35\%$. The average temperatures of grinding media are 298.051 K, 298.053 K, 298.056 K, 298.057 K, 298.057 K, and 298.055 K. The temperature field of grinding media under higher grinding media filling is more inhomogeneous than that of a lower grinding media filling. The reason for this is that the collision frequency and the contact number increase with the grinding media filling, so the grinding media temperature rises increases. As the grinding media filling continues to increase, the bulk of the grinding media is very close to the center of the mill and contributes little to the

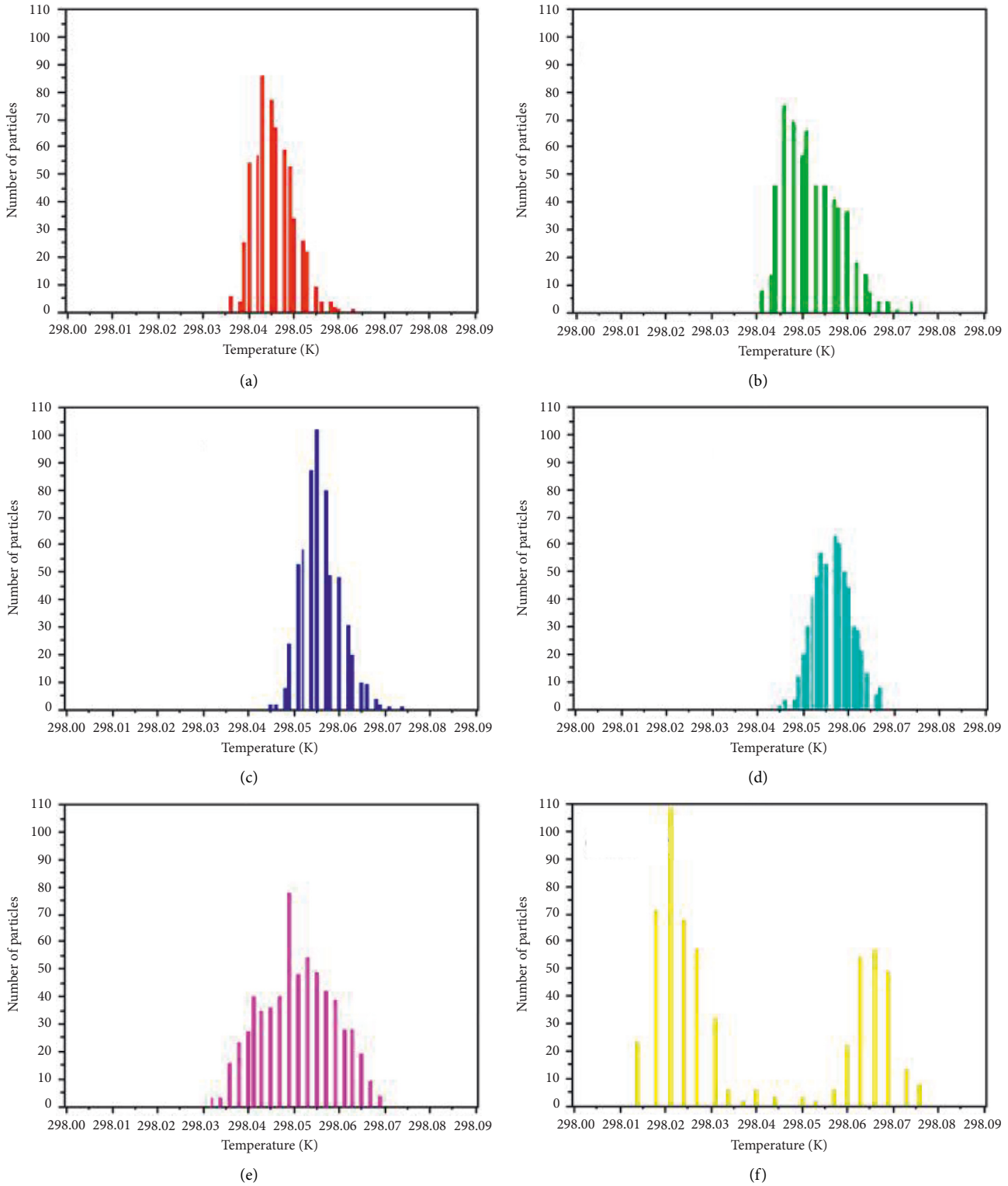

Figure 3: The distributions of grinding media temperatures for different mill speeds. (a) $\psi = 50\%$. (b) $\psi = 60\%$. (c) $\psi = 70\%$. (d) $\psi = 80\%$. (e) $\psi = 90\%$. (f) $\psi = 100\%$.

grinding media being off-center. Therefore, the grinding media contributes little to the temperature rise. This result indicates that the grinding media temperature varies slightly with the increase of the grinding media filling.

4.3. Effect of Number of Lifters. Lifters are generally used to raise grinding media to transfer the energy from a mill to a load. The distribution of the lifters around a mill shell is an essential factor that affects the grinding and crushing

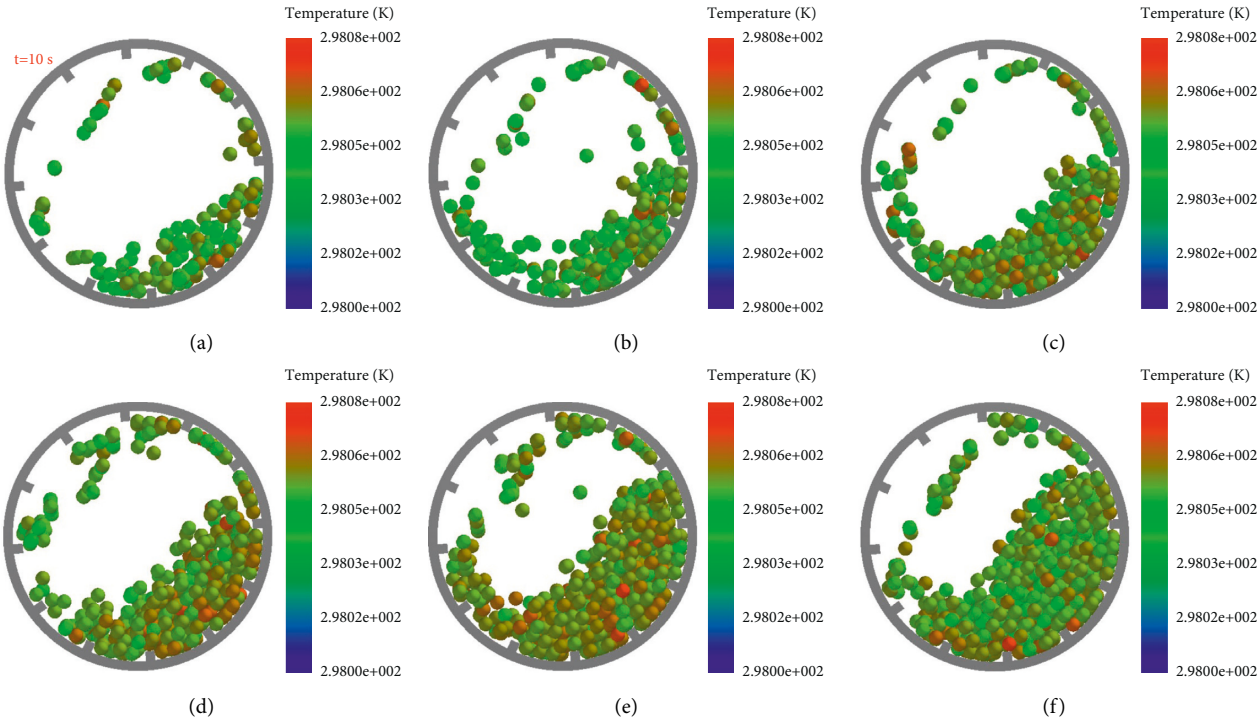

Figure 4: Effect of grinding media filling on the grinding media temperature field. (a) $J = 10\%$. (b) $J = 15\%$. (c) $J = 20\%$. (d) $J = 25\%$. (e) $J = 30\%$. (f) $J = 35\%$.

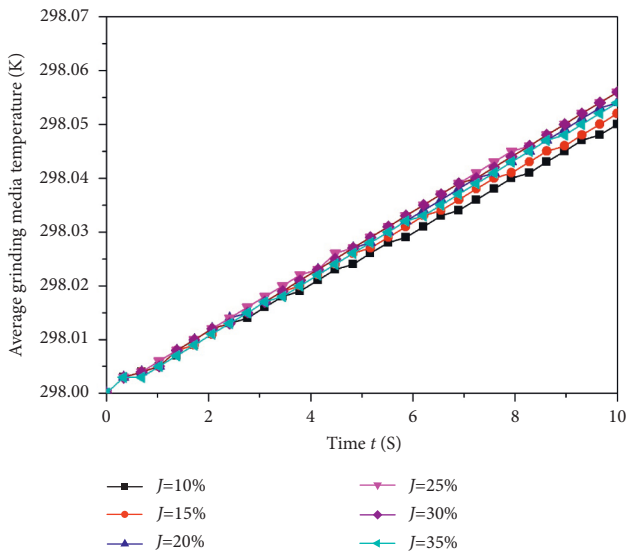

Figure 5: The distributions of grinding media temperatures for different grinding media fillings.

efficiency. To understand the interrelation between the number of lifters and the temperature field of grinding media, for the ball mill, the number of lifters for four levels is selected to be between $n = 0$ and $n = 16$, as shown in Figure 6. The results showed that the shoulder angle of grinding media increases with the number of lifters. However, the temperature field of grinding media revealed that the heat transfer increases first and then decreases. With the number of lifters $n = 0$, all the grinding media is located in the cascading regime, and the grinding media is piled together to grind each other. The temperature field of grinding media is more uniform. With the number of lifters $n = 8$, a fraction of grinding media is lifted, but the distribution of the grinding media temperature field changes relatively minor compared with $n = 0$. With the number of lifters $n = 12$, increasing the number of lifters cause more grinding media to be lifted, and the temperature field of grinding media shows the highest temperature rise. This is because the lifter hinders the sliding motion of the grinding media and promotes the cataracting movement. With the number of lifters $n = 16$, the excessive number of lifters increases the slippage between grinding media. This indicates that the distance between two lifters restricts the sliding motion and accelerates the cataracting movement.

Figure 7 shows the distribution of the grinding media temperature field for the different number of lifters, which corresponds to Figure 6. It can be seen that the maximum particle number corresponding to the temperatures of grinding media are 298.048 K, 298.051 K, 298.057 K, and 298.056 K, respectively. The average temperature of grinding media reaches a maximum value of 295.057 K at $n = 12$. However, the average temperature of grinding media reaches a minimum value of 298.047 K at $n = 0$. These results indicated that increasing the number of lifters can improve heat transfer.

5. Comparison with DEM Simulation and Experiment

The laboratory-scale ball mill with two detachable acrylic plates is employed to validate the established heat transfer model. As shown in Figure 8, the experimental setup consists

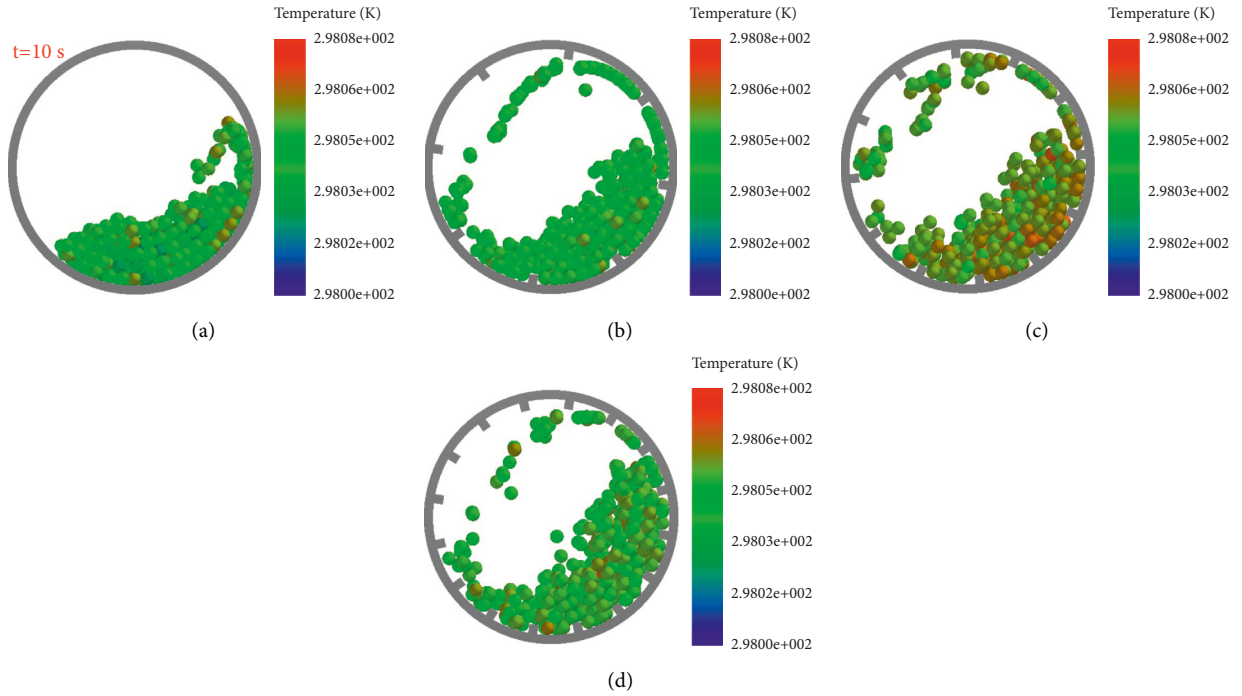

Figure 6: Effect of the number of lifters on grinding media temperature field. (a) $n = 0$. (b) $n = 8$. (c) $n = 12$. (d) $n = 16$.

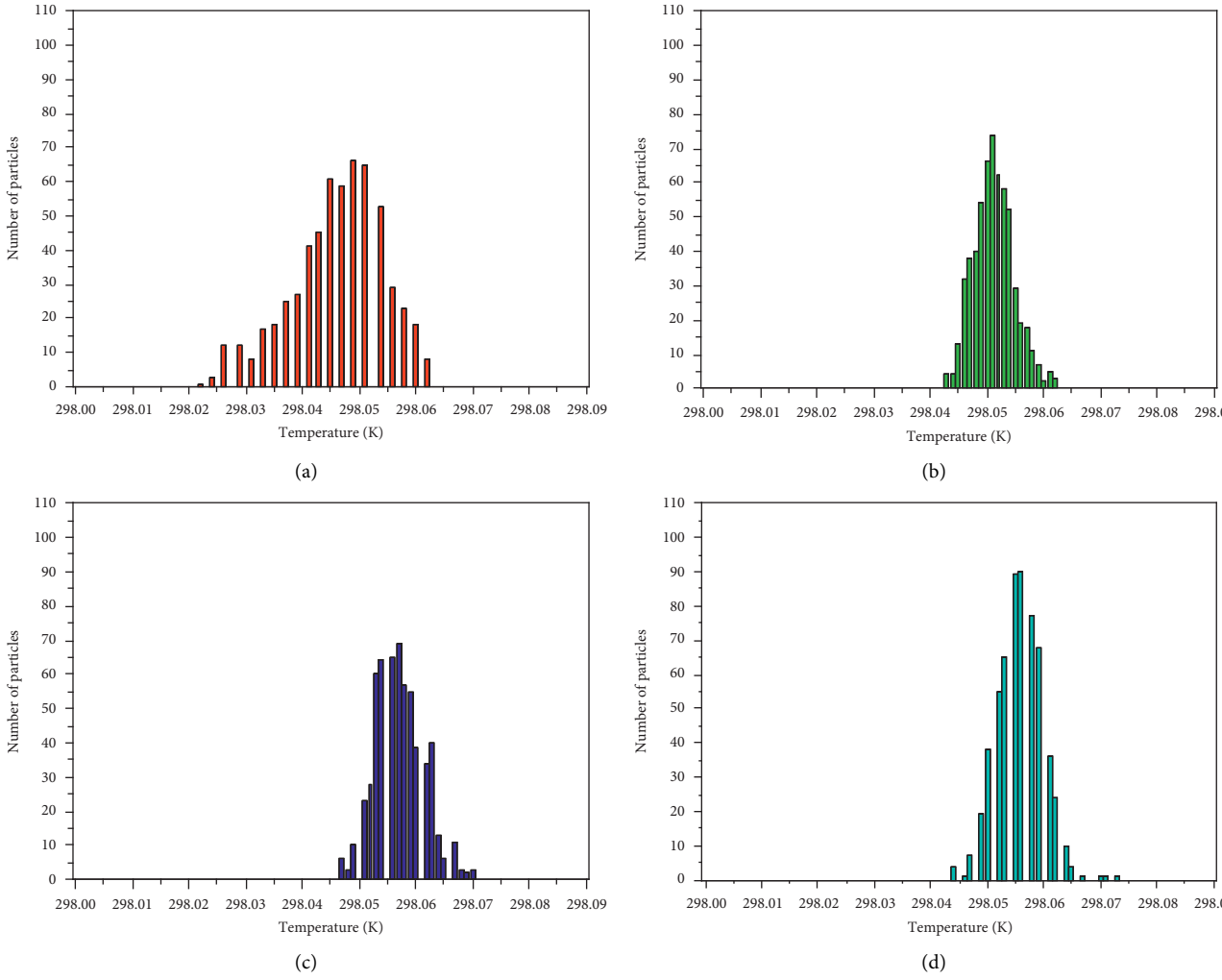

Figure 7: The distributions of grinding media temperature for different numbers of lifters. (a) $n = 0$. (b) $n = 8$. (c) $n = 12$. (d) $n = 16$.

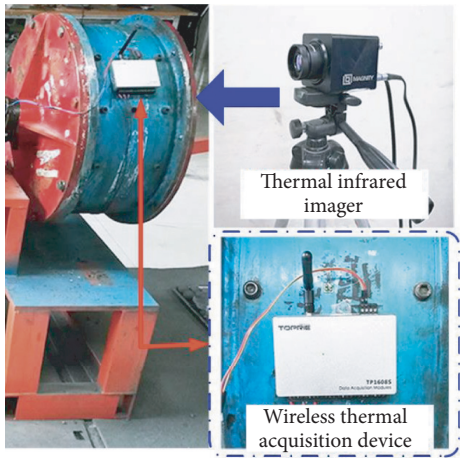

Figure 8: Laboratory-scale ball mill.

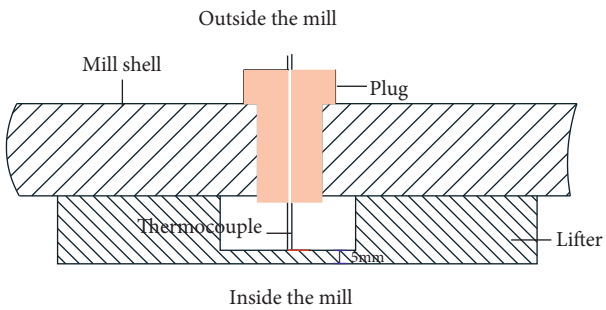

Figure 9: Schematic diagram of thermocouple installation.

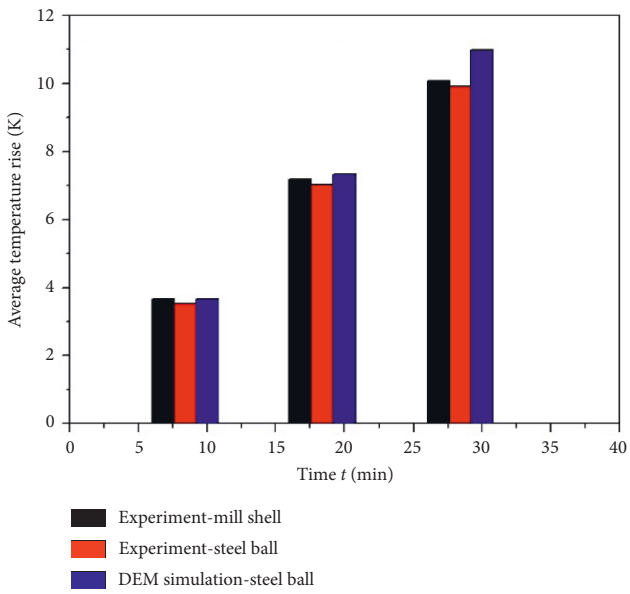

Figure 10: Comparison of temperature rise between DEM simulation and experiment.

of a wireless thermal device and a thermal infrared imager. A high-precision wireless thermal acquisition device is used to measure the mill shell temperature. The measuring accuracy is 0.2% and can realize the online temperature measurement. The mill shell temperature was measured by the thermocouple and the installation method of the thermocouple on the mill shell as shown in Figure 9. A combination of contact and noncontact methods is used to determine the emissivity of the steel ball. The results show an emissivity of 0.96 for the steel balls. The thermal infrared imager is used to measure the temperature of the steel ball, with a measuring accuracy of 2%. In the experiments, the ball mill is stopped at predetermined intervals to open the mill shell quickly and then photograph the steel ball using a thermal infrared imager. The grinding durations are $t = 0$ min, $t = 10$ min, $t = 20$ min, and $t = 30$ min.

One set of validation tests is used to validate the numerical simulations. The experiments are carried out with a mill speed of 75% of the critical speed, a grinding media filling of 25%, and a steel ball size of 30 mm. Figure 10 shows the average temperature rise of the steel ball for the DEM simulations and the experimental results. Since the DEM simulation time is limited, the results are calculated proportionally. As shown in Figure 10, the DEM simulation results agree with the experimental results, despite the former being slightly higher. The primary reason for this discrepancy is that the temperature dissipation produced by mill shutdown is ignored. In addition, only the temperature on the surface of the grinding media is measured by the thermal infrared imager, which makes this error acceptable. In summary, the rationality of the numerical model of heat transfer is well validated by the experimental results.

6. Conclusions

This study mainly investigates the effect of the mill speed, grinding media filling, and the number of lifters on the discrete heat transfer behavior of grinding media in ball mills. In DEM simulations, the temperature field of grinding media and the load behavior is susceptible to the mill speed, grinding media filling, and the number of lifters. The average temperature of the grinding media firstly increases and then decreases with the increased mill speed, grinding media filling, and the number of lifters. Consequently, the developed heat transfer model is well-validated, and the temperature field of the grinding media is in good agreement with the experimental results, indicating the reasonableness and reliability of the model. The numerical models of heat transfer provide an opportunity to optimize the movement and mixing of granular materials sensitive to temperature.

Data Availability

The data used to support the findings of this study are included within the article.

Conflicts of Interest

The authors declare that there are no conflicts of interest.

Authors' Contributions

The authors wish to thank Yin for conceiving and designing the schemes; Wang and Li performed the experiments and analyzed the data.

Acknowledgments

This study was supported by the Doctoral Scientific Research Foundation of Suzhou University (Grant no. 2020BS004) and the National Natural Science Foundation of China (Grant no. 51475458). The authors also wish to thank the Natural Science Foundation of the Jiangsu Higher Education Institutions of China (Grant no. 19KJB440004), the Natural Science Research Project in Universities of Anhui Province in China (Grant no. KJ2021A1115), and the Nature Science Research Key Project of Suzhou University (Grant no. 2019yzd03).

References

[1] G. W. Delaney, P. W. Cleary, R. D. Morrison, S. Cummins, and B Loveday, "Predicting breakage and the evolution of rock size and shape distributions in Ag and SAG mills using DEM," *Minerals Engineering*, vol. 50-51, no. 5, pp. 132–139, 2013.

[2] N. S. Weerasekara, M. S. Powell, P. W. Cleary et al., "The contribution of DEM to the science of comminution," *Powder Technology*, vol. 248, no. 248, pp. 3–24, 2013.

[3] M. Yahyaei and S. Banisi, "Spreadsheet-based modeling of liner wear impact on charge motion in tumbling mills," *Minerals Engineering*, vol. 23, no. 15, pp. 1213–1219, 2010.

[4] Z. X. Yin, Y. X. Peng, Z. C. Zhu, Z. Yu, and T Li, "Impact load behavior between different charge and lifter in a laboratory-scale mill," *Materials*, vol. 10, no. 8, p. 882, 2017.

[5] C. H. Liu, W. Cai, M. Y. Zhai, G. Zhu, C. Zhang, and Z Jiang, "Decoupling of wastewater eco-environmental damage and China's economic development," *Science of the Total Environment*, vol. 789, Article ID 147980, 2021.

[6] P. W. Cleary and R. D. Morrison, "Understanding fine ore breakage in a laboratory scale ball mill using DEM," *Minerals Engineering*, vol. 24, no. 3–4, pp. 352–366, 2011.

[7] Y. X. Peng, T. Q. Li, Z. C. Zhu, S. Zou, and Z Yin, "Discrete element method simulations of load behavior with mono-sized iron ore particles in a ball mill," *Advances in Mechanical Engineering*, vol. 9, no. 5, Article ID 168781401770559, 2017.

[8] T. Q. Li, Y. X. Peng, Z. C. Zhu et al., "Multi-layer kinematics and collision energy in a large-scale grinding mill-the largest semi-autogenous grinding mill in China," *Advances in Mechanical Engineering*, vol. 8, no. 12, Article ID 168781401668137, 2016.

[9] V. V. R. Natarajan and M. L. Hunt, "Kinetic theory analysis of heat transfer in granular flows," *International Journal of Heat and Mass Transfer*, vol. 41, no. 13, pp. 1929–1944, 1998.

[10] E. E. Michaelides, "Heat transfer in particulate flows," *International Journal of Heat and Mass Transfer*, vol. 29, no. 2, pp. 265–273, 1986.

[11] J. R. Ferron and D. K. Singh, "Rotary kiln transport processes," *AIChE Journal*, vol. 37, no. 5, pp. 747–758, 1991.

[12] C. A. Cook and V. A. Cundy, "Heat transfer between a rotating cylinder and a moist granular bed," *International Journal of Heat and Mass Transfer*, vol. 38, no. 3, pp. 419–432, 1995.

[13] M. L. Hunt, "Discrete element simulations for granular material flows: effective thermal conductivity and self-diffusivity," *International Journal of Heat and Mass Transfer*, vol. 40, no. 13, pp. 3059–3068, 1997.

[14] Y. Kaneko, T. Shiojima, and M. Horio, "DEM simulation of fluidized beds for gas-phase olefin polymerization," *Chemical Engineering Science*, vol. 54, no. 24, pp. 5809–5821, 1999.

[15] J. Li and D. J. Mason, "A computational investigation of transient heat transfer in pneumatic transport of granular particles," *Powder Technology*, vol. 112, no. 3, pp. 273–282, 2000.

[16] W. L. Vargas and J. J. Mccarthy, "Unsteady heat conduction in granular materials[J]," *Mrs Proceedings*, vol. 627, no. 5, pp. 1052–1059, 2000.

[17] I. Skuratovsky, A. Levy, and I. Borde, "Two-dimensional numerical simulations of the pneumatic drying in vertical pipes," *Chemical Engineering and Processing: Process Intensification*, vol. 44, no. 2, pp. 187–192, 2005.

[18] B. Chaudhuri, F. J. Muzzio, and M. S. Tomassone, "Experimentally validated computations of heat transfer in granular materials in rotary calciners," *Powder Technology*, vol. 198, no. 1, pp. 6–15, 2010.

[19] Q. Xie, Z. B. Chen, Q. F. Hou, A. Yu, and R Yang, "DEM investigation of heat transfer in a drum mixer with lifters," *Powder Technology*, vol. 314, pp. 175–181, 2017.

[20] H. Komossa, S. Wirtz, V. Scherer, F. Herz, and E Specht, "Heat transfer in indirect heated rotary drums filled with monodisperse spheres: Comparison of experiments with DEM simulations," *Powder Technology*, vol. 286, pp. 722–731, 2015.

[21] N. Gui and J. R. Fan, "Numerical study of heat conduction of granular particles in rotating wavy drums," *International Journal of Heat and Mass Transfer*, vol. 84, pp. 740–751, 2015.

[22] I. Figueroa, W. L. Vargas, and J. J. McCarthy, "Mixing and heat conduction in rotating tumblers," *Chemical Engineering Science*, vol. 65, no. 2, pp. 1045–1054, 2010.

[23] T. Oschmann, M. Schiemann, and H. Kruggel-Emden, "Development and verification of a resolved 3D inner particle heat transfer model for the Discrete Element Method (DEM)," *Powder Technology*, vol. 291, pp. 392–407, 2016.

[24] M. Y. Li, X. Ling, H. Peng, Z. Cao, and Y Wang, "An investigation on heat transfer of granular materials in the novel flighted rotary drum," *Canadian Journal of Chemical Engineering*, vol. 95, no. 2, pp. 386–397, 2017.

[25] V. D. Nguyen, C. Cogné, M. Guessasma, E. Bellenger, and J Fortin, "Discrete modeling of granular flow with thermal transfer: application to the discharge of silos," *Applied Thermal Engineering*, vol. 29, no. 8-9, pp. 1846–1853, 2009.

[26] X. X. Duan and Y. J. Cao, *Theory and Practice of ball mill*, Metallurgical Industry Press, Beijing, 1999.

[27] T. Q. Li, Z. X. Yin, and G. Y. Wu, "Study on heat transfer behavior and thermal breakage characteristic of the charge in ball mills," *Advances in Mechanical Engineering*, vol. 13, no. 3, Article ID 168781402199496, 2021.

[28] S. Rosenkranz, S. Breitung-Faes, and A. Kwade, "Experimental investigations and modelling of the ball motion in planetary ball mills," *Powder Technology*, vol. 212, no. 1, pp. 224–230, 2011.